Kinetic Turbulence in Laboratory, Space, and Astrophysical Plasmas

A renewal request for an XSEDE Research Allocation

by Gregory G. Howes (University of Iowa)

1. Introduction and Scientific Background

This request for computational resources through XSEDE supports four separate but complementary projects on the topic of turbulence in laboratory, space, and astrophysical plasmas. Although the science questions to be addressed by each of the topics differ, in many cases data from a single simulation can be used in several of the proposed projects, so this proposal will focus on the simulations to be performed using XSEDE resources, with an abridged discussion of the science issues to be addressed by each proposed simulation. Below we provide a brief introduction to each of the projects and the science questions to be addressed with the proposed simulations.

1.1 Using Field-Particle Correlations to Diagnose the Dissipation of Plasma Turbulence Plasma turbulence occurs ubiquitously throughout the heliosphere, yet our understanding of how turbulence governs energy transport and plasma heating remains incomplete, constituting a grand challenge problem in heliophysics. Specifically, we have yet to determine definitively the kinetic physical mechanisms responsible for the damping of the turbulent electromagnetic fluctuations in the weakly collisional solar wind and the ultimate conversion of their energy into plasma heat. In weakly collisional heliospheric plasmas, such as the solar corona and solar wind, damping of the turbulent fluctuations occurs due to collisionless interactions between the electromagnetic fields and the individual plasma particles. If there is a net transfer of energy from the electromagnetic fields to the microscopic motion of the particles, it will necessarily lead to correlations between the fields and the fluctuations in the particle velocity distributions. This project aims to develop a completely new technique to apply field-particle correlations to single-point measurements to provide a direct measure of the energy transfer associated with the collisionless damping of the turbulent fluctuations in the solar wind.

Performing nonlinear gyrokinetic simulations of astrophysical plasma turbulence using the Astrophysical Gyrokinetics Code, `AstroGK` [29], we will generate single-point time series of the electromagnetic fields $\mathbf{E}$ and $\mathbf{B}$ and the full 2D gyrokinetic distribution function $\delta f_s(v_\parallel, v_\perp)$ at a number of points spread throughout the simulation domain. The fluctuations in these turbulent fields will be correlated to provide a measure of the net transfer of energy from the turbulent fluctuations to the microscopic motion of the particles. Ultimately, testing these field-particle correlations using nonlinear gyrokinetic simulations will enable us to refine the technique for application to the analysis of spacecraft measurements of turbulence in the solar wind and the solar corona (when the upcoming NASA *Solar Probe Plus* mission becomes the first manmade object to penetrate the outer regions of the corona). This powerful field-particle correlation technique has the potential to transform our ability to measure the plasma heating and particle acceleration caused by the dissipation of turbulence. This project is funded by both a CAREER Award through the Solar and Terrestrial program of the NSF Division of Atmospheric and Geospace Sciences and a recently renewed NSF-DOE Partnership in Plasma Physics grant.

1.2 Development of Magnetic Field Line Wander in Plasma Turbulence The magnetic field in the heliosphere and other more distant astrophysical plasmas is not smooth and straight, but rather is frequently observed to be tangled up in a complicated way, most likely due to the turbulent motions of the plasma. As one travels along a single magnetic field line, neighboring field lines can wander away, possibly with their separation increasing exponentially. This tangling of the magnetic field impacts the transport of energetic particles (cosmic rays and solar energetic particles) [22, 37, 44, 45, 49, 43, 11, 12, 13] and may also play an important role in the turbulent cascade of energy to small scales [46, 26, 42].

Developing a detailed understanding of how the magnetic field gets tangled in a turbulent plasma is a new direction of my research program. This project began supported by funds from my recently completed

PECASE Award through the NASA Solar and Heliospheric Physics program, and is now supported by my NSF CAREER Award through the Solar and Terrestrial program of the NSF Division of Atmospheric and Geospace Sciences and an NSF Graduate Research Fellowship to my graduate student Jennifer Verniero. Theoretical arguments suggest that the dynamics of the turbulence are primarily responsible for the tangling of the magnetic field, and magnetic reconnection enables tangled magnetic field lines to break and ultimately become untangled. As long as the electron scales are fully resolved, our gyrokinetic simulations accurately reproduce the kinetic physics of magnetic reconnection in comparison to Particle-In-Cell (PIC) simulations [51].

We propose to employ driven simulations of Alfvén wave turbulence at the small-scale end of the inertial range to understand the balance between the tangling of the field by the turbulent motions and the untangling of the field by magnetic reconnection. The key approach is to compare nonlinear gyrokinetic simulations using `AstroGK`, in which the small-scale kinetic dynamics of collisionless magnetic reconnection are resolved, to reduced MHD simulations of the turbulence using the `Gandalf` GPU code, in which the reconnection of the magnetic field is due solely to resistive effects. This comparison will enable us to determine if the specific mechanism of reconnection—collisionless reconnection in the gyrokinetic case, and resistive reconnection in the reduced MHD case—alters the development and evolution of the magnetic field line wander.

1.3 Auroral Electron Acceleration by Inertial Alfvén Waves The physics of the aurora is one of the foremost unsolved problems of space physics. The mechanisms responsible for accelerating electrons that precipitate onto the ionosphere are not fully understood. For more than three decades, particle interactions with Alfvén waves have been proposed as a possible means for accelerating electrons and generating aurorae. Here we propose gyrokinetic simulations to be performed to support both the experimental design and the analysis of laboratory measurements in coordination with an experimental program to study this mechanism of auroral electron acceleration in the Large Plasma Device (LAPD) at UCLA. This project is funded jointly by a recently renewed NSF-DOE Partnership in Plasma Physics grant and an NSF Graduate Research Fellowship to graduate student James Schroeder.

The use of field-particle correlations (see Sec. 1.1) to diagnose the energy transfer between electromagnetic field and individual plasma particles is an important new approach to diagnose the acceleration of electrons under auroral conditions. Using this new technique, we can employ nonlinear `AstroGK` simulations of inertial Alfvén waves to simulate the acceleration of electrons. The results will enable us to design an experiment and devise experimentally measurable signatures of the acceleration of electrons by inertial Alfvén waves, relevant to the dynamics in the Earth's polar magnetosphere. A number of runs with high resolution in both physical space and velocity space are necessary to provide theoretical predictions with which to compare our experimental measurements of accelerated electrons in the tail of the distribution function using the novel Whistler Wave Absorption Diagnostic [47, 55] in the LAPD plasma.

1.4 Application of Bispectral Analysis to Understand Energy Transfer and Current Sheet Generation in Plasma Turbulence Our recent comprehensive and coordinated program of analytical [19], numerical [28, 20], and experimental [18, 8] investigations of plasma turbulence has established that the nonlinear interaction between perpendicularly polarized, counterpropagating Alfvén waves—commonly referred to as an "Alfvén wave collision"—represents the fundamental building block of astrophysical plasma turbulence. `AstroGK` simulations using our 2014 and 2015 XSEDE allocations have enabled us to show the exciting new result that strong Alfvén wave collisions appear to self-consistently generate small-scale current sheets in the plasma. These current sheets are ubiquitously observed in plasma turbulence using solar wind observations [32, 5, 34, 33, 36, 57, 59, 31] and numerical simulations [56, 23, 52, 59, 61, 60], but the physical mechanism responsible for generating these current sheets had previously been unknown.

To delve further into the details of the nonlinear interactions that are responsible for the development of these current sheets, we aim to employ the powerful approach of *bispectral analysis*. In this approach, the

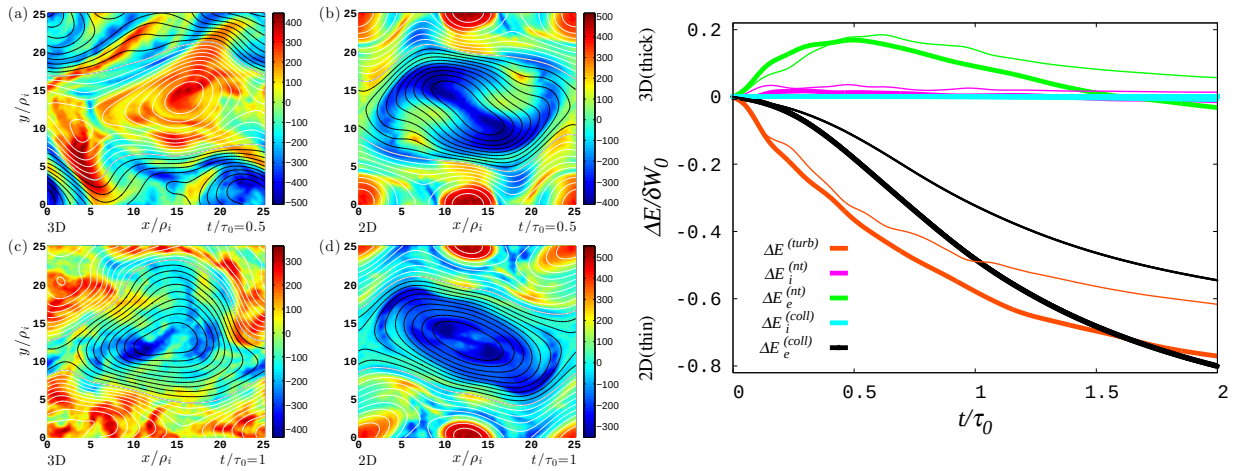

Figure 1: (Left) Spatial profile of J_z (color) and $A_\parallel$ (contours) on the $z = 0$ plane of the OTV3D (left) and OTV2D (right) simulations at $t/\tau_0 = 0.5$ (top) and $t/\tau_0 = 1$ (bottom). Contours represent positive (white) and negative (black) values of $A_\parallel$. (Right) Change of energy over total initial fluctuating energy, $\Delta E/\delta W_0$, for the turbulent energy $E^{(turb)}$ (orange), the non-thermal energy $E_s^{(nt)}$ of ions (magenta) and electrons (green), the collisionally dissipated energy $E_s^{(coll)}$ for ions (cyan) and electrons (black). Line thickness indicates OTV3D (thick) or OTV2D (thin) simulations.

nonlinear energy transfer between different modes in the plasma can be computed using the bispectrum, a correlation of three separate spatial magnetic field modes, $\langle \delta B_y(\mathbf{k}_1, t_1)\delta B_x(\mathbf{k}_2, t_2)\delta B_x(\mathbf{k}_1 + \mathbf{k}_2, t_3)\rangle$. Unfortunately, this analysis is computationally very *heavy*, requiring a significant amount of data to compute. The best approach is to compute this information *on the fly*, during the simulation itself, to avoid having to save large amounts of data from the simulation. Thus, we are working on *in situ* diagnostics that will be compute the bispectrum during the turbulence simulation itself. The aim is to identify the small number of modes that play the key role both in mediating the nonlinear energy transfer to small scales and in governing the development of coherent structures in the form of current sheets. This project is funded by both a CAREER Award through the Solar and Terrestrial program of the NSF Division of Atmospheric and Geospace Sciences.

2. Progress Report on Results from Previous XSEDE Allocations

[Note that this section is identical to the separate, required "Progress Report" document.]

In this section, we review the progress from the previous use of the XSEDE Research Allocation TG-PHY090084, *Kinetic Turbulence in Laboratory, Space, and Astrophysical Plasmas*. Although the `AstroGK` numerical simulations performed using the XSEDE allocation have contributed to a number of submitted or published studies, we focus here on three of the most exciting results and accomplishments: (i) differences and similarities in the nonlinear energy transfer and dissipation of turbulence in 2D and 3D simulations, (ii) spatially localized dissipation that occurs within current sheets that are self-consistently developed as a result of Alfvén wave collisions, and (iii) the development of stochastic magnetic fields in plasma turbulence. The simulation results shown here were produced using either *Stampede* at the Texas Advanced Computing Center or *Darter* at the National Institute for Computational Science.

2.1 Energy Flow and Dissipation in 2D and 3D Plasma Turbulence One of the key questions addressed by the "Turbulence Dissipation Challenge," [35] a community effort supported by the NSF Solar, Heliospheric, and INterplanetary Environment (SHINE) program, is whether the physical mechanisms of dissipation are the same in 2D and 3D simulations. Following moderate spatial resolution simulations using our

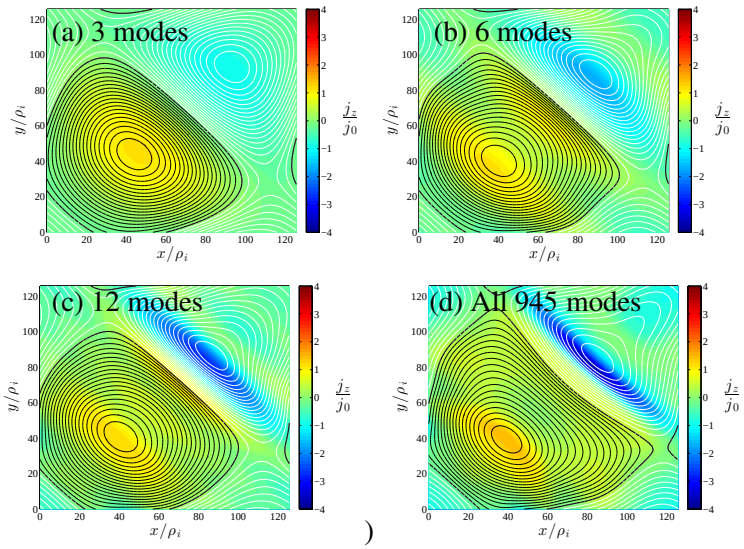

Figure 2: Normalized current j_z/j_0 (colorbar) and contours of parallel vector potential $A_\parallel$ (positive–black, negative–white) in the perpendicular plane from an `AstroGK` simulation of a strong Alfvén wave collision. Filtering is used to remove all but the select number of Fourier modes shown in each panel. Constructive interference among just 12 perpendicular Fourier modes (c) reproduces qualitatively the current sheet arising in the full simulation of a strong Alfvén wave collision (d).

)

2014 XSEDE allocation, we employed a substantial fraction of our 2015 XSEDE allocation to perform high resolution $(n_x, n_y, n_z, n_\lambda, n_\varepsilon, n_s) = (128, 128, 32, 32, 32, 2)$ simulations of with three values of ion plasma beta, $\beta_i = 1$, $\beta_i = 0.1$, and $\beta_i = 0.01$. The key goal was to explore the qualitative differences for the nonlinear turbulent cascade and the damping of the turbulence between the 2D and 3D simulations.

Figure 1 shows some of the results from these simulations. We use the standard 2D Orszag-Tang Vortex (OTV) problem [30] and a particular 3D extension of the OTV problem that was devised for this project [25]. The four panels on the left show a perpendicular (to the mean magnetic field) cross-section of the turbulence in the 3D (left) and 2D (right) simulations at $t/\tau_0 = 0.5$ (top) and $t/\tau_0 = 1$ (bottom), where τ is the "eddy-turnaround time" at the simulation domain scale. The rightmost panel shows the time evolution of the different components of the energy for both 3D and 2D simulations for the $\beta_i = 0.01$ case (relevant to the conditions in the solar corona). The results demonstrate the intriguing finding that, although the turbulent cascade occurs more rapidly (and thus leads to more rapid dissipation of the initial turbulent energy) in the 3D case (thick lines), the qualitative nature of the dissipation is the same in both 3D and 2D cases. Additional analysis examining the velocity space structure of the energy transfer suggests that Landau damping is the physical mechanism of dissipation in both cases, even though it is widely believed that Landau damping cannot occur in the 2D case (this view turns out to be wrong). These exciting new results are currently under review with *Physical Review Letters*.

2.2 Current Sheets and Dissipation in Astrophysical Plasma Turbulence The cutting edge of research on the turbulence in space and astrophysical plasmas currently focuses on the kinetic mechanisms for the damping of turbulent motions and the resulting plasma heating in the weakly collisional solar wind. Current spacecraft missions, such as *Cluster*, sample the plasma with sufficient time resolution to explore the turbulence at length scales at or below the ion Larmor radius, $k\rho_i \gtrsim 1$, in the "dissipation range" of solar wind turbulence [41, 24, 3, 6, 40, 2]. In particular, the space physics community is now poised to answer the question, "What physical mechanisms are responsible for the dissipation of the plasma turbulence in the solar wind?" Of course, the answer to this question depends strongly on the nature of the small-scale fluctuations in the dissipation range of the solar wind.

In the past few years, vigorous activity has focused on the inherent development of coherent structures in plasma turbulence, particularly current sheets with widths down to the scale of the electron Larmor radius, and the role played by such structures in the dissipation of kinetic plasma turbulence [32, 34, 33, 56, 23, 59, 52, 53]. A wide body of numerical simulations of plasma turbulence, from fluid to kinetic simulations, finds the development of thin current sheets at smallest resolved scales as the turbulence evolves. But

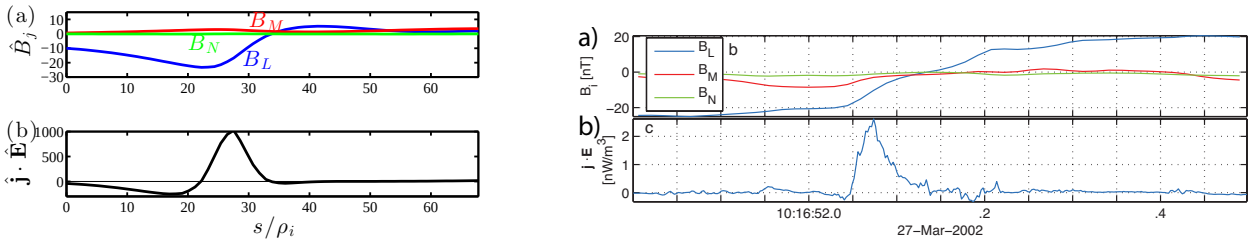

Figure 3: (Left) Profile along trajectory through the current sheet in Fig. 7 (black line). (a) Magnetic field components rotated to minimum variance coordinates [48] (b) Measure of the dissipation rate of the current sheet $\mathbf{j} \cdot \mathbf{E}$ along the trajectory. From Howes 2015 [15]. (Right) Measurements of a current sheet in the Earth's turbulent magnetosheath, with (a) the magnetic field in minimum variance coordinates and (b) the dissipation rate of the current sheet $\mathbf{j} \cdot \mathbf{E}$. From Sundkvist *et al.* 2007 [50].

one key question remains unanswered, "What process leads to the formation of these current sheets in plasma turbulence?" Using our 2015 XSEDE allocation, we completed a set of simulations of Alfvén wave collisions [19, 28, 20, 18, 8] to confirm that the current sheets are self-consistently generated as a consequence of the nonlinear interactions in Alfvén wave collisions in the strong turbulence limit.

In Figure 2, we show the current sheet that develops in a strong Alfvén wave collision simulation filtered by the number of Fourier modes necessary to describe the current sheet. We find that, due to our new understanding of the nonlinear energy transfer in Alfvén wave collisions (an understanding developed with extensive use of XSEDE computing resources), it takes very few Fourier modes to reproduce the current sheet, and the amplitude and phase of each of those modes can be analytically predicted. Therefore, these results suggest that a simple mechanism—the nonlinear interaction between counterpropagating Alfvén waves—is responsible for the development of the ubiquitously observed current sheets in plasma turbulence.

Furthermore, in Figure 3 (left), we plot a slice through the current sheet in Figure 2(d) (along the line $x = y$) to show that the energy transfer from the turbulent electromagnetic fields to the particles is indeed localized to the region near the current sheet, consistent with spacecraft observations of a turbulent current sheet in the Earth's magnetosheath (right) [38, 50].

2.3 Development of Stochastic Magnetic Field Lines in Plasma Turbulence The tangling of the magnetic field in turbulent astrophysical plasmas has not generally been a focus of previous plasma turbulence investigations, but the complicated topology of the magnetic field observed in turbulence simulations significantly impacts the transport of energetic particles (cosmic rays and solar energetic particles) [22, 37, 44, 45, 49, 43, 11, 12, 13] and may also play an important but under-appreciated role in the turbulent cascade of energy to small scales [46, 26, 42].

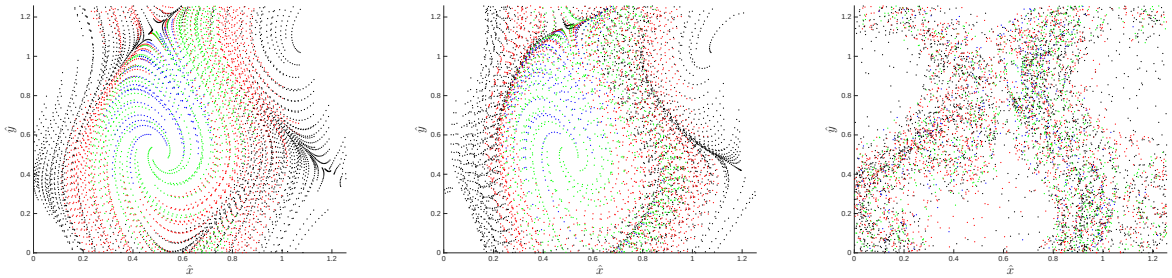

Figure 4: Development of stochasticity in plasma turbulence driving from smooth initial conditions. At $t = 0.342t_A$ (left), distorted field lines still describe relatively smooth flux surfaces. At $t = 0.522t_A$ (center), regions of the plot begin to take on a stochastic appearance. By $t = 1.422t_A$ (right), the turbulently wandering magnetic field has become completely stochastic, corresponding to the destruction of the nested magnetic flux surfaces that provide confinement in a toroidal geometry [39, 9, 37].

We used our 2015 XSEDE allocation to perform simulations of driven kinetic Alfvén wave turbulence to examine how the magnetic field lines transition from being smooth to stochastic. The development of stochasticity in the turbulent magnetic field as a function of time can be investigated using Poincaré recurrence plots of the positions of individual magnetic field lines each time they pass through the periodic boundary along the equilibrium magnetic field direction [7, 27, 58]. Figure 4 shows the progression of the simulation with ion plasma beta $\beta_i = 1$ and nonlinearity parameter $\chi = 1$, where the wandering of the magnetic field lines transitions to a stochastic character at around $t = 0.5t_A$, where t_A is the Alfvén wave crossing time in the equilibrium field direction. We have performed a suite of simulations with $\beta_i = 1$ over a wide range of different driving amplitudes (covering a range from very strong $\chi = 4$ to very weak $\chi = 1/16$ driving). Our work has shown for the first time that there does indeed appear to be a threshold at $\chi \gtrsim 1/8$ to yield the transition to stochasticity shown in Figure 4; weaker turbulence with $\chi < 1/8$ does not lead to stochastic magnetic field lines.

3. Proposed Simulations

In this section, we briefly describe the numerical algorithms employed by the Astrophysical Gyrokinetics Code `AstroGK`, and we outline the specific numerical simulations that we propose to perform on XSEDE resources during the next year. Note that core counts in the following estimates do not reflect the need for total cores to be a multiple of 16 for *Stampede*—when a job is run, we use the next highest multiple of 16. For example, a 1892-core job will request 1904 cores (119 16-core nodes), but use only 1892 cores, leading to an acceptably small 0.6% inefficiency. Also, to keep the allocation estimates simple, we state our needs strictly in terms of *Stampede* hours—**we can alternatively use an equivalent number of hours on *Darter*, or some combination thereof**.

3.1 Simulation Code `AstroGK` The simulations proposed here will be performed using `AstroGK`, the Astrophysical Gyrokinetics Code, developed specifically to study kinetic turbulence in astrophysical plasmas. A detailed description of the code and the results of linear and nonlinear benchmarks are presented in [29], so we give here only a brief overview.

`AstroGK` evolves the perturbed gyroaveraged distribution function $h_s(k_x, k_y, z, \lambda, \varepsilon)$ for each species s, the scalar potential φ, parallel vector potential $A_\parallel$, and the parallel magnetic field perturbation $\delta B_\parallel$ according to the gyrokinetic equation and the gyroaveraged Maxwell's equations [10, 16]. The velocity space coordinates are $\lambda = v_\perp^2/v^2$ and $\varepsilon = v^2/2$. The domain is a periodic box of size $L_\perp^2 \times L_\parallel$, elongated along the straight, uniform mean magnetic field B_0. Note that, in the gyrokinetic formalism, all quantities may be rescaled to any parallel dimension satisfying $L_\parallel/L_\perp \gg 1$. Uniform Maxwellian equilibria for ions (protons) and electrons are chosen, and the correct mass ratio $m_i/m_e = 1836$ is used. Spatial dimensions (x, y) perpendicular to the mean field are treated pseudo-spectrally; an upwind finite-difference scheme is used in the parallel direction, z. Collisions are incorporated using a fully conservative, linearized collision operator that includes energy diffusion and pitch-angle scattering [1, 4]. An operator splitting scheme is employed to advance the linear, nonlinear, and collision terms using different algorithms. The linear and collision terms are advanced using an implicit, Beam-Warming algorithm, leading to relaxation of the very stringent timestep constraint on the parallel electron motion that would be necessary using an explicit scheme. The nonlinear term employs an explicit 3rd-order Adams-Bashforth scheme, and indeed must satisfy a CFL criterion for stability, but one that is significantly less restrictive than that for the linear electron dynamics. The code employs a flexible parallelization scheme, supporting different layouts of the data for decomposition, enabling efficient performance for significantly different computational problems.

`AstroGK` enables similar simulations to be run concurrently in a single submitted job (embarrassingly parallel, so no performance degradation). For example, a suite of four runs, each employing 1024 cores, can be run as a single submitted job with 4096 cores, but the parallel performance for each simulation in the suite is still that of a run with 1024 cores. This strategy helps to make effective use of large computing

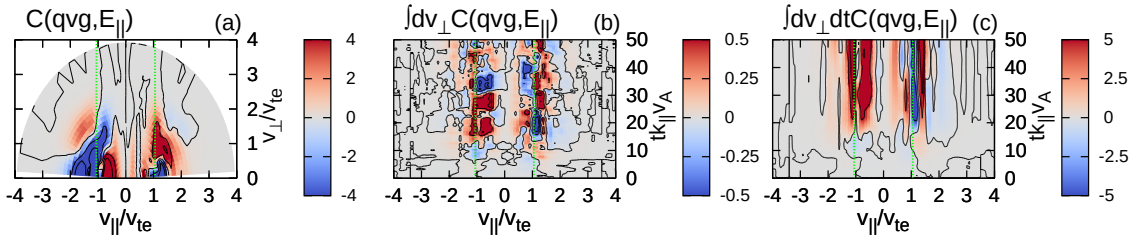

Figure 5: (a) Correlation over the $(v_\parallel, v_\perp)$ plane. (b) Plot of the reduced correlation $C_\tau\left(q_i v_\parallel \delta g_i(\mathbf{x}_0, v_\parallel, t), E_\parallel(\mathbf{x}_0, t)\right)$ for a correlation time $\tau = 2/k_\parallel v_A$. (c) Time-integrated change in the energy density $\delta w_i(\mathbf{x}_0, v_\parallel) = \int_0^t C(v_\parallel, t', \tau) dt'$.

allocations.

3.2 Field-Particle Correlations in Plasma Turbulence Project 1.1 (see Section 1.1) employs driven simulations of plasma turbulence. The capability for producing plasma turbulence simulations that reproduce the energy spectrum of turbulence in the solar wind with our antenna driving mechanism [54] is well documented by our previous work [17, 14, 21, 52, 53] (all supported by NSF XSEDE resources). For this project, we will compute the field-particle correlation from the distribution function $g(v_\parallel)$ and electric field data, given by the reduced correlation

$$C(v_\parallel, t, \tau) = C_\tau\left(q_s v_\parallel \delta g_s(\mathbf{x}_0, v_\parallel, t), E_\parallel(\mathbf{x}_0, t)\right) \tag{1}$$

An example of the results of this correlation, applied to moderate resolution `AstroGK` simulations computed with our 2015 XSEDE allocation, is shown in Figure 5.

We aim to perform two separate driven turbulence simulations: (i) one simulation focusing on ion dissipation, with $\beta_i = 1$ and a fully resolved range of scales $0.1 \leq k_\perp \rho_i \leq 4.2$; and (ii) one simulation focusing on electron dissipation, with $\beta_i = 0.1$ and a fully resolved range of scales $2.5 \leq k_\perp \rho_i \leq 105$. Therefore, The simulation domain for the ion simulation is $L_{\perp i}^2 \times L_{\parallel i} = (20\pi\rho_i)^2 \times 20\pi\rho_i/\epsilon$ and for the electron simulation is $L_{\perp e}^2 \times L_{\parallel e} = (4\pi\rho_i/5)^2 \times 4\pi\rho_i/5\epsilon$. The wave period for the outer scale of the ion simulation is $\tau_{Ai} = L_{\parallel i}/(2\pi v_A)$ and for the electron simulation is $\tau_{Ae} \simeq L_{\parallel e}/(5\pi v_A)$.

We choose high resolution $(n_x, n_y, n_z, n_\lambda, n_\varepsilon, n_s) = (128, 128, 32, 64, 64, 2)$ for each of the two 5D gyrokinetic simulations for this project. The two simulations will be run concurrently on 2048 cores each, for a total of 4096 cores per submitted job. To perform the time-averaging necessary to perform the field-particle correlations to isolate the net ion or electron heating, we need to evolve the simulations for at least three outer scale wave periods $3\tau_{As}$.

Tests have shown that the timesteps for the ion dissipation simulation is $1 \times 10^{-5}\tau_{Ai}$ and for the electron simulation is $1.1 \times 10^{-5}\tau_{Ae}$ (these are approximately the same since the dealiased perpendicular dynamic of both simulations is approximately 42—in our estimates we will take both timesteps to be $1 \times 10^{-5}\tau_{As}$, where s denotes the species). To evolve the simulations for $3\tau_{As}$ requires $300,000$ steps, at a measured time per step of 12.8 s on Stampede.

# Cores	Steps/run	Time/step (s)	Wallclock/run (h)	# Runs	Total SUs
4096 (2048×2)	300,000	12.8	1066	1 (2 simulations each)	4,400,000

We plan to perform 46 restarts requiring 23 h wallclock time each and utilizing 4096 cores per job.

3.3 Development of Magnetic Field Line Wander in Plasma Turbulence After having used our 2015 XSEDE Allocation to determine that the stochastic tangling of the magnetic field has a threshold value for small-scale kinetic Alfvén wave turbulence (in which the untangling of the field is accomplished by resolved

collisionless magnetic reconnection [51]), we now want to determine if the mechanism of reconnection alters the untangling of the magnetic field. To do this, we will compare nonlinear gyrokinetic simulations using `AstroGK` with nonlinear reduced MHD simulations using the `Gandalf` GPU code. Reduced MHD is a 3D fluid model and is far less computationally demanding than the 5D gyrokinetic simulations, but its dissipation by reconnection is not physically accurate with respect to weakly collisional space and astrophysical plasmas. However, the GPU code can be run on a single GPU, and so no resources are necessary to perform the comparison runs proposed here. Below we just describe the computational requirements for the nonlinear gyrokinetic simulations using `AstroGK`.

To ensure that the physics of collisionless magnetic reconnection is resolved in our simulations (which requires the electron scales to be resolved), we choose to run our simulations with a reduced mass ratio $m_i/m_e = 9$, meaning that the scale of reconnection will occur at $k_\perp \rho_e = 1$, or $k_\perp \rho_i = 3$. We choose resolution to achieve a fully resolved range of scales $0.1 \leq k_\perp \rho_i \leq 4.2$. The physics of magnetic reconnection is highly dependent on the ion plasma beta, so we choose two values, $\beta_i = 1$ and $\beta_i = 0.01$. For each value of β_i, we will run simulations with a range of turbulent amplitudes, with the nonlinearity parameter varying over $\chi \in [0.0625, 0.25, 1, 4]$. Thus, this project requires a suite of 8 simulations.

The 5D simulation dimensions for each simulation are $(n_x, n_y, n_z, n_\lambda, n_\varepsilon, n_s) = (128, 128, 64, 32, 32, 2)$ The eight simulations will be run concurrently using 1024 cores each, for a total of 8192 cores per submitted job. For these simulations, we need to run for at least four outer scale times, $4\tau_A$, to observe how the tangling of the magnetic field evolves and saturates. To evolve each simulation for four outer scale times requires 270,000 steps at a timestep of $1.5 \times 10^{-5}\tau_A$. The measured time per step on Stampede using 1024 cores per simulation is 5.4 s. The eight simulations will be run concurrently using 1024 cores each, for a total of 8192 cores per submitted job.

# Cores	Steps/run	Time/step (s)	Wallclock/run (h)	# Runs	Total SUs
8192 (1024×8)	270,000	5.4	405	1 (8 simulations each)	3,300,000

We plan to perform 18 restarts requiring 22 h wallclock time each and utilizing 8192 cores per job.

3.4 Electron Acceleration Simulations We have recently developed and fully tested novel diagnostics in `AstroGK` for examining the signatures of collisionless wave-particle interactions on the velocity distributions of ions and electrons (see Sec 2.2). In these simulations, we initialize an inertial Alfvén wave (the "kinetic" small-scale extension of the Alfvén wave in the limit of very low ion plasma beta, $\beta_i < m_e/m_p \sim 5 \times 10^{-4}$) and observe the development of structure in velocity space of electrons as the wave propagates and undergoes resonant collisionless wave-particle interactions (Landau damping) with the electrons in the tail of the velocity distribution.

The spatial resolution for these runs need only be moderate, but high resolution in velocity space is essential, so we take simulation dimensions of $(n_x, n_y, n_z, n_\lambda, n_\varepsilon, n_s) = (32, 32, 128, 32, 32, 2)$. We hope to perform this simulation for two values $\beta_i = 2 \times 10^{-4}$ and $\beta_i = 5 \times 10^{-5}$, for a total of two simulations to be run concurrently using 1892 cores each, for a total of 3784 cores per submitted job. For a timestep of $5 \times 10^{-5}\tau_A$, one crossing time requires approximately $125,000$ steps, at a measured time per step of $0.87\ s$ from preliminary runs on Stampede. We aim to run at least four crossing times, for a total of $500,000$ steps.

# Cores	Steps/run	Time/step (s)	Wallclock/run (h)	# Runs	Total SUs
3784 (1892×2)	500,000	0.87	121	1 (2 simulations each)	500,000

We plan to perform 6 restarts requiring 22 h wallclock time each and utilizing 3784 cores per job.

3.5 Bispectral Analysis of Plasma Turbulence To compute a bispectrum of turbulence data,

$$\langle \delta B_y(\mathbf{k}_1, t_1) \delta B_x(\mathbf{k}_2, t_2) \delta B_x(\mathbf{k}_1 + \mathbf{k}_2, t_3) \rangle \tag{2}$$

we need to correlate the measurements of the magnetic field at different times. For the application to understand the nonlinear energy transfer between different modes in the plasma, we will typically have $t_1 = t_2$, and the third time t_3 will be shifted from t_1 by some phase of the wave (typically one-quarter of the wave-period for this problem). Therefore, we need to run simulations where we can compute the product $B_y(\mathbf{k}_1, t_1)\delta B_x(\mathbf{k}_2, t_1)$ and save it to multiply by $\delta B_x(\mathbf{k}_1 + \mathbf{k}_2, t_3)$ at some later time t_3. This can be done relatively efficiently *in situ* (during the turbulence simulation), without having to save a large amount of the data to disk.

To do this, we need to re-run our simulations with the diagnostic turned on. But, since the results of this analysis are not expected to change with the plasma parameters, we can do this for just one simulation to get the insight we want. We choose to perform an Alfvén wave collision simulation [28] (similar to those run using our 2014 and 2015 XSEDE allocation) with $\beta_i = 1$ in the MHD Alfvén wave regime with $L_\perp^2 \times L_\parallel = (40\pi\rho_i)^2 \times 40\pi\rho_i/\epsilon$. The resolution is $(n_x, n_y, n_z, n_\lambda, n_\varepsilon, n_s) = (128, 128, 64, 32, 32, 2)$, and the timestep is $5 \times 10^{-6}\tau_A$ with the bispectral diagnostics running. To run two Alfvén wave crossing times, $2\tau_A$, we require $400,000$ steps, at a measured time per step of $6.4\ s$ on Stampede.

# Cores	Steps/run	Time/step (s)	Wallclock/run (h)	# Runs	Total SUs
2048	400,000	6.4	711	1	1,400,000

We plan to perform 32 restarts requiring 22 h wallclock time each and utilizing 2048 cores per job.

3.6 Request Summary The request summary for resources on Stampede at TACC follows:

Section	Total SUs
3.2	4,400,000
3.3	3,300,000
3.4	500,000
3.5	1,400,000
Total SUs Requested	9,600,000

Note that although we are officially requesting that all of this time be granted on Stampede at TACC, we could use an equivalent amount of time on Darter at NICS instead, or some combination thereof.

4. Management

In addition to my own group at the University of Iowa (PI Prof. Greg Howes, postdocs Dr. Tak Chu Li and Dr. Sofiane Bourouaine, and NSF Graduate Research Fellows James Schroeder and Jennifer Verniero, and graduate student Andrew McCubbin), these projects include collaborations with a number of separate research groups at institutions throughout the United States and abroad, including: UCLA (Prof. Troy Carter) and University of Iowa (Prof. Craig Kletzing and Prof. Fred Skiff) for the study of electron acceleration by inertial Alfvén waves in the laboratory, funded by the NSF-DOE Partnership in Plasma Physics; the University of New Hampshire (Dr. Kris Klein) and University of Michigan (Prof. Justin Kasper) for the study of field-particle correlations in plasma turbulence; University of Maryland (Prof. Bill Dorland), UC Berkeley (Prof. Eliot Quataert), University of Oxford in the UK (Prof. Alex Schekochihin and Dr. Michael Barnes), University of Hyogo in Japan (Prof. Ryusuke Numata), and University of Electro-Communications in Tokyo (Prof. Tomo Tatsuno) for a study of the fundamental physics of kinetic turbulence and its dissipation in space and astrophysical plasmas, funded by the PI's NSF CAREER Award through the Solar Terrestrial Program of the Atmospheric and Geospace Sciences at NSF.

PI Gregory Howes has a share of Helium, a 3600-core shared HPC cluster at the University of Iowa. This local computational resource is ideal for exploratory runs and small-scale parameter scans to identify the best parameters for the large-scale runs proposed here.

Progress Report

Here we review the progress from the previous use of the XSEDE Research Allocation TG-PHY090084, *Kinetic Turbulence in Laboratory, Space, and Astrophysical Plasmas* using either *Stampede* at the Texas Advanced Computing Center or *Darter* at the National Institute for Computational Science.

2.1 Energy Flow and Dissipation in 2D and 3D Plasma Turbulence One of the key questions addressed by the "Turbulence Dissipation Challenge," [35] a community effort supported by the NSF Solar, Heliospheric, and INterplanetary Environment (SHINE) program, is whether the physical mechanisms of dissipation are the same in 2D and 3D simulations. Following moderate spatial resolution simulations using our 2014 XSEDE allocation, we employed a substantial fraction of our 2015 XSEDE allocation to perform high resolution $(n_x, n_y, n_z, n_\lambda, n_\varepsilon, n_s) = (128, 128, 32, 32, 32, 2)$ simulations of with three values of ion plasma beta, $\beta_i = 1$, $\beta_i = 0.1$, and $\beta_i = 0.01$. The key goal was to explore the qualitative differences for the nonlinear turbulent cascade and the damping of the turbulence between the 2D and 3D simulations.

Figure 1 shows some of the results from these simulations. We use the standard 2D Orszag-Tang Vortex (OTV) problem [30] and a particular 3D extension of the OTV problem that was devised for this project [25]. The four panels on the left show a perpendicular (to the mean magnetic field) cross-section of the turbulence in the 3D (left) and 2D (right) simulations at $t/\tau_0 = 0.5$ (top) and $t/\tau_0 = 1$ (bottom), where τ is the "eddy-turnaround time" at the simulation domain scale. The rightmost panel shows the time evolution of the different components of the energy for both 3D and 2D simulations for the $\beta_i = 0.01$ case (relevant to the conditions in the solar corona). The results demonstrate the intriguing finding that, although the turbulent cascade occurs more rapidly (and thus leads to more rapid dissipation of the initial turbulent energy) in the 3D case (thick lines), the qualitative nature of the dissipation is the same in both 3D and 2D cases. Additional analysis examining the velocity space structure of the energy transfer suggests that Landau damping is the physical mechanism of dissipation in both cases, even though it is widely believed that Landau damping cannot occur in the 2D case (this view turns out to be wrong). These exciting new results are currently under review with *Physical Review Letters*.

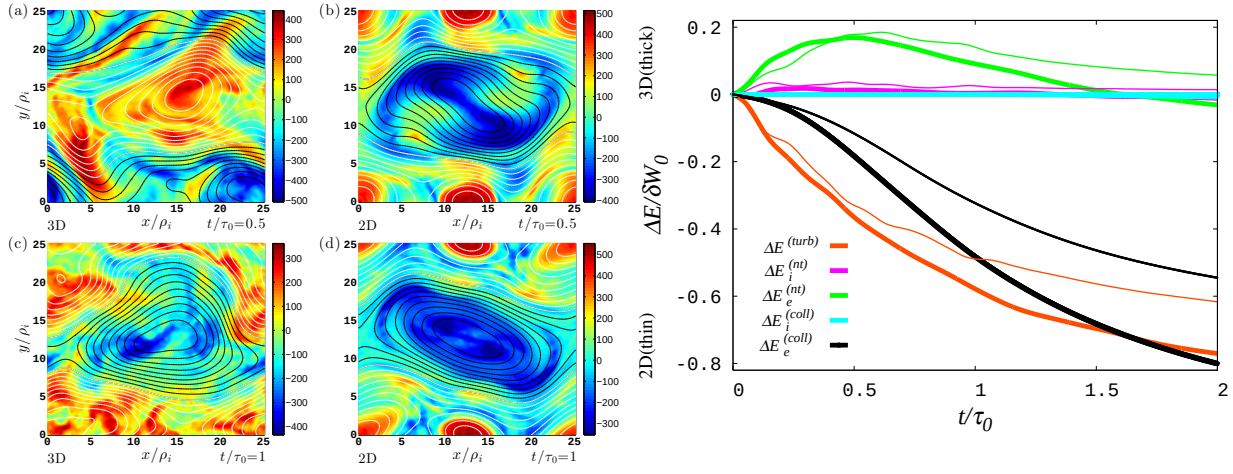

Figure 1: (Left) Spatial profile of J_z (color) and $A_\parallel$ (contours) on the $z = 0$ plane of the OTV3D (left) and OTV2D (right) simulations at $t/\tau_0 = 0.5$ (top) and $t/\tau_0 = 1$ (bottom). Contours represent positive (white) and negative (black) values of $A_\parallel$. (Right) Change of energy over total initial fluctuating energy, $\Delta E/\delta W_0$, for the turbulent energy $E^{(turb)}$ (orange), the non-thermal energy $E_s^{(nt)}$ of ions (magenta) and electrons (green), the collisionally dissipated energy $E_s^{(coll)}$ for ions (cyan) and electrons (black). Line thickness indicates OTV3D (thick) or OTV2D (thin) simulations.

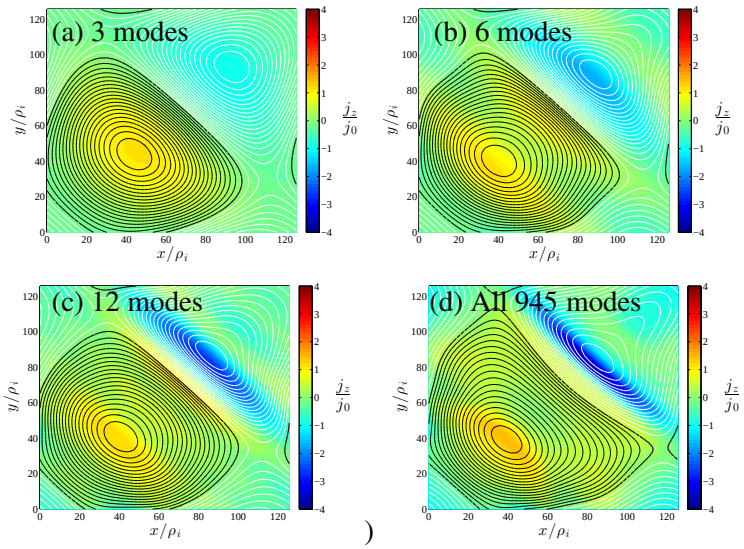

Figure 2: Normalized current j_z/j_0 (colorbar) and contours of parallel vector potential $A_\parallel$ (positive–black, negative–white) in the perpendicular plane from an `AstroGK` simulation of a strong Alfvén wave collision. Filtering is used to remove all but the select number of Fourier modes shown in each panel. Constructive interference among just 12 perpendicular Fourier modes (c) reproduces qualitatively the current sheet arising in the full simulation of a strong Alfvén wave collision (d).

)

2.2 Current Sheets and Dissipation in Astrophysical Plasma Turbulence The cutting edge of research on the turbulence in space and astrophysical plasmas currently focuses on the kinetic mechanisms for the damping of turbulent motions and the resulting plasma heating in the weakly collisional solar wind. Current spacecraft missions, such as *Cluster*, sample the plasma with sufficient time resolution to explore the turbulence at length scales at or below the ion Larmor radius, $k\rho_i \gtrsim 1$, in the "dissipation range" of solar wind turbulence [41, 24, 3, 6, 40, 2]. In particular, the space physics community is now poised to answer the question, "What physical mechanisms are responsible for the dissipation of the plasma turbulence in the solar wind?" Of course, the answer to this question depends strongly on the nature of the small-scale fluctuations in the dissipation range of the solar wind.

In the past few years, vigorous activity has focused on the inherent development of coherent structures in plasma turbulence, particularly current sheets with widths down to the scale of the electron Larmor radius, and the role played by such structures in the dissipation of kinetic plasma turbulence [32, 34, 33, 56, 23, 59, 52, 53]. A wide body of numerical simulations of plasma turbulence, from fluid to kinetic simulations, finds the development of thin current sheets at smallest resolved scales as the turbulence evolves. But one key question remains unanswered, "What process leads to the formation of these current sheets in plasma turbulence?" Using our 2015 XSEDE allocation, we completed a set of simulations of Alfvén wave collisions [19, 28, 20, 18, 8] to confirm that the current sheets are self-consistently generated as a consequence of the nonlinear interactions in Alfvén wave collisions in the strong turbulence limit.

In Figure 2, we show the current sheet that develops in a strong Alfvén wave collision simulation filtered by the number of Fourier modes necessary to describe the current sheet. We find that, due to our new understanding of the nonlinear energy transfer in Alfvén wave collisions (an understanding developed with extensive use of XSEDE computing resources), it takes very few Fourier modes to reproduce the current sheet, and the amplitude and phase of each of those modes can be analytically predicted. Therefore, these results suggest that a simple mechanism—the nonlinear interaction between counterpropagating Alfvén waves—is responsible for the development of the ubiquitously observed current sheets in plasma turbulence.

Furthermore, in Figure 3 (left), we plot a slice through the current sheet in Figure 2(d) (along the line $x = y$) to show that the energy transfer from the turbulent electromagnetic fields to the particles is indeed localized to the region near the current sheet, consistent with spacecraft observations of a turbulent current sheet in the Earth's magnetosheath (right) [38, 50].

2.3 Development of Stochastic Magnetic Field Lines in Plasma Turbulence The tangling of the magnetic field in turbulent astrophysical plasmas has not generally been a focus of previous plasma turbu-

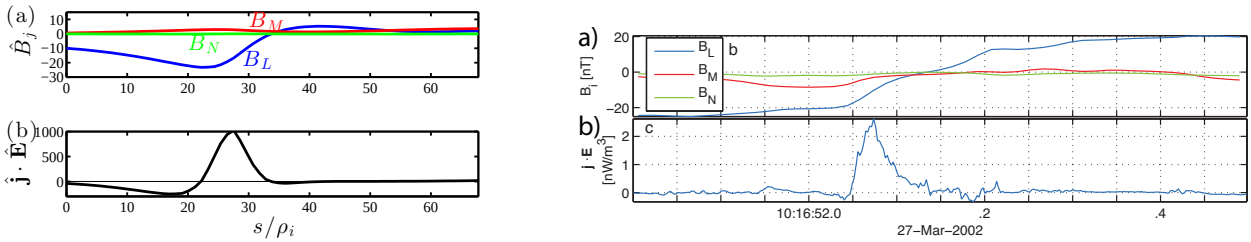

Figure 3: (Left) Profile along trajectory through the current sheet in Fig. 7 (black line). (a) Magnetic field components rotated to minimum variance coordinates [48] (b) Measure of the dissipation rate of the current sheet $\mathbf{j} \cdot \mathbf{E}$ along the trajectory. From Howes 2015 [15]. (Right) Measurements of a current sheet in the Earth's turbulent magnetosheath, with (a) the magnetic field in minimum variance coordinates and (b) the dissipation rate of the current sheet $\mathbf{j} \cdot \mathbf{E}$. From Sundkvist *et al.* 2007 [50].

lence investigations, but the complicated topology of the magnetic field observed in turbulence simulations significantly impacts the transport of energetic particles (cosmic rays and solar energetic particles) [22, 37, 44, 45, 49, 43, 11, 12, 13] and may also play an important but under-appreciated role in the turbulent cascade of energy to small scales [46, 26, 42].

We used our 2015 XSEDE allocation to perform simulations of driven kinetic Alfvén wave turbulence to examine how the magnetic field lines transition from being smooth to stochastic. The development of stochasticity in the turbulent magnetic field as a function of time can be investigated using Poincaré recurrence plots of the positions of individual magnetic field lines each time they pass through the periodic boundary along the equilibrium magnetic field direction [7, 27, 58]. Figure 4 shows the progression of the simulation with ion plasma beta $\beta_i = 1$ and nonlinearity parameter $\chi = 1$, where the wandering of the magnetic field lines transitions to a stochastic character at around $t = 0.5t_A$, where t_A is the Alfvén wave crossing time in the equilibrium field direction. We have performed a suite of simulations with $\beta_i = 1$ over a wide range of different driving amplitudes (covering a range from very strong $\chi = 4$ to very weak $\chi = 1/16$ driving). Our work has shown for the first time that there does indeed appear to be a threshold at $\chi \gtrsim 1/8$ to yield the transition to stochasticity shown in Figure 4; weaker turbulence with $\chi < 1/8$ does not lead to stochastic magnetic field lines.

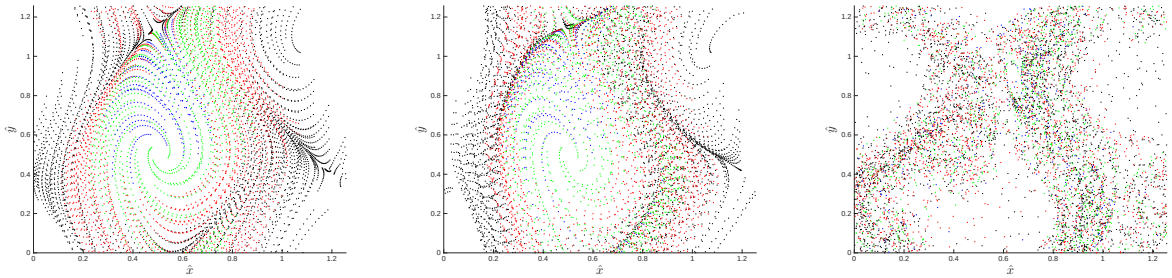

Figure 4: Development of stochasticity in plasma turbulence driving from smooth initial conditions. At $t = 0.342t_A$ (left), distorted field lines still describe relatively smooth flux surfaces. At $t = 0.522t_A$ (center), regions of the plot begin to take on a stochastic appearance. By $t = 1.422t_A$ (right), the turbulently wandering magnetic field has become completely stochastic, corresponding to the destruction of the nested magnetic flux surfaces that provide confinement in a toroidal geometry [39, 9, 37].

Code Performance and Scaling

1.0 Parallel Performance Scaling Parallel performance of `AstroGK` is measured by taking the weak and strong scalings: The weak scaling is probed by holding the computational work per processing core constant while the number of cores, thus the total problem size, is increased. On the other hand, the strong scaling is probed by holding the problem size constant while the number of processing cores is increased. Both tests are performed on Stampede Dell PowerEdge Cluster at the Texas Advanced Computing Center (TACC). At the time these scaling tests were performed, `Stampede` consisted of 6400 compute nodes, each node consisting of 16 processing cores (two Xeon E5-2680 8-core processors) and one 61-core Intel Xeon Phi SE10P Coprocessor. The coprocessors were not used for these scaling tests.

1.1 Weak Scaling The initial problem uses $(N_x, N_y, N_Z, N_\lambda, N_E, N_s) = (160, 160, 36, 6, 4, 2)$ on 16 processing cores (one node). Each time the processing core count is doubled, the problem size is doubled by alternately doubling first N_E and then N_λ—since both of these dimensions scale linearly with the problem size, doubling one of these dimensions effectively doubles the computational work, leading to fair assessment of the weak scaling. The weak scaling behavior of the wallclock time per step $t_{\rm step}$ vs. the number of processing cores up to $N_{\rm proc} = 4096$ is plotted in Fig. 1. `AstroGK` achieves nearly ideal scaling over the entire range of problem sizes tested, with a slight degradation in perfomance at the highest problem size. The layout specified for the parallel communication for this test is `'yxles'`.

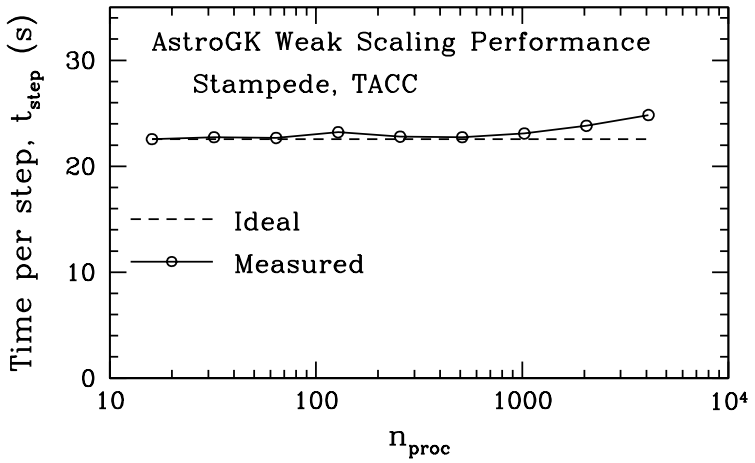

Figure 1: Weak scaling of `AstroGK` determined by holding the computational work per processor constant while the number of processors is increased. The time per step $t_{\rm step}$ vs. the number of processing cores $N_{\rm proc}$ is plotted.

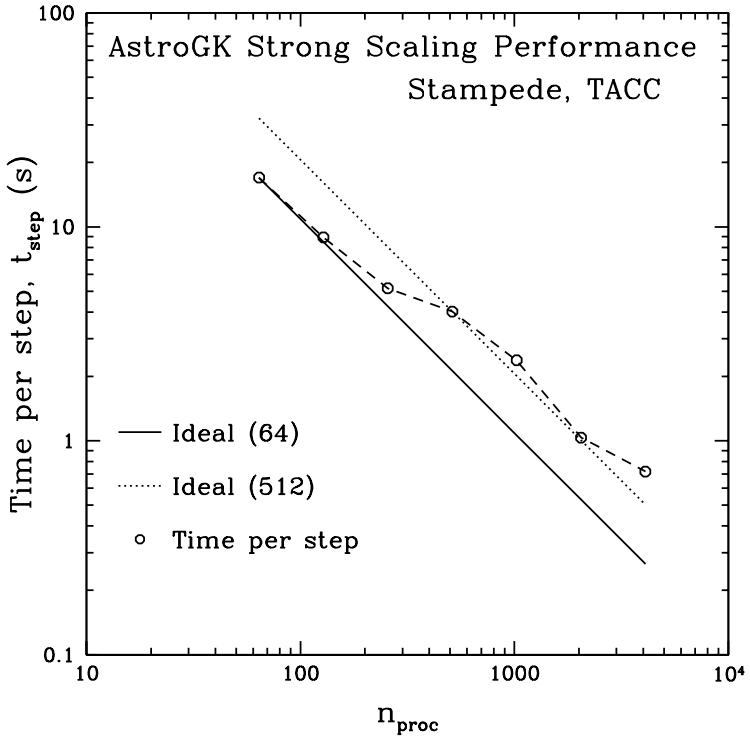

Figure 2: Plot of strong scaling taken by increasing the number of processors for the fixed problem size. The time per step $t_{\rm step}$ vs. the number of processors $N_{\rm proc}$ is shown. Ideal linear scaling lines compared with $N_{\rm proc} = 64$ and $N_{\rm proc} = 512$ are depicted.

1.2 Strong Scaling The dimensions of the nonlinear turbulence problem employed for this scaling are $(N_x, N_y, N_Z, N_\lambda, N_E, N_s) = (32, 32, 24, 192, 256, 2)$. The strong scaling behavior of the wallclock time per step $t_{\rm step}$ vs. the number of processors $N_{\rm proc}$ is plotted from $N_{\rm proc} = 64$ to $N_{\rm proc} = 4096$ in Fig. 2. Again, the layout specified for the parallel communication is $'$`yxles`$'$.

To accommodate this large computational problem on a small number of processors requires more memory per core than is available when all 16 cores on a compute node are used. Therefore, for the lowest three data points on the scaling curve (up to 512 processors), only 2, 4, and 8 cores are utilized per node. The rest of the runs utilize all 16 cores per node. As the number of cores per node increases, the computation time deviates from the ideal linear scaling ("Ideal (64)" line in the figure). The sharing of communication and memory bandwidth between multiple cores lead to a factor of two degradation of performance. If the number of cores per node is fixed at 16, we observe a nearly ideal strong scaling from $N_{\rm proc} = 512$ up to $N_{\rm proc} = 2048$, as indicated by "Ideal(512)" line in the figure. A slight degradation in performance occurs only at $N_{\rm proc} = 4096$.

Publications Resulting from XSEDE Support

Published papers resulting from XSEDE support:

1. *Using Field-Particle Correlations to Investigate the Dissipation of Plasma Turbulence*
   Klein, K. G., **Howes, G. G.**, and Li, T. C.
   Phys. Rev. Lett., submitted (2016).

2. *Diagnosing Collisionless Energy Transfer Using Field-Particle Correlations: Vlasov-Poisson Plasmas*
   Howes, G. G., Klein, K. G., and Li, T. C.
   J. Plasma Phys., submitted (2016).

3. *The Development of Current Sheets in Astrophysical Plasma Turbulence*
   Howes, G. G.
   Phys. Rev. Lett., submitted (2016).

4. *Dissipation via Landau Damping in Two- and Three-Dimensional Plasma Turbulence*
   Li, T. C., **Howes, G. G.**, Klein, K. G., and TenBarge, J. M.
   Phys. Rev. Lett., submitted (2015).

5. *A dynamical model of plasma turbulence in the solar wind*
   Howes, G. G.
   Phil. Trans. Roy. Soc. A, **373**,20140145 [28 pages] (2015).

6. *Kinetic Turbulence*
   Howes, G. G.
   in *Magnetic Fields in Diffuse Media*, ed. by E. de Gouveia Dal Pino and A. Lazarian,
   Springer: Heidelberg [29 pages] (2015).

7. *Collisionless Reconnection in the Large Guide Field Regime: Gyrokinetic Versus Particle-in-Cell Simulations*
   TenBarge, J. M., Daughton, W., Karimabadi, H., **Howes, G. G.**, and Dorland, W.
   Phys. Plasmas, **21**, 020708 [5 pages] (2014).

8. *An Oscillating Langevin Antenna for Driving Plasma Turbulence Simulations*
   TenBarge, J. M., **Howes, G. G.**, Dorland, W., and Hammett, G. W.
   Comp. Phys. Comm., **185**, 578 [12 pages] (2014).

9. *Collisionless Damping at Electron Scales in Solar Wind Turbulence*
   TenBarge, J. M., **Howes, G. G.** and Dorland, W.
   Astrophys. J., **774**, 139 [10 pages] (2013).

10. *Alfven Wave Collisions, The Fundamental Building Block of Plasma Turbulence I: Asymptotic Solution*
    Howes, G. G. and Nielson, K. D.
    Phys. Plasmas, **20**, 072302 [19 pages] (2013).

11. *Alfven Wave Collisions, The Fundamental Building Block of Plasma Turbulence II: Numerical Solution*
    Nielson, K. D., **Howes, G. G.** and Dorland, W.
    Phys. Plasmas, **20**, 072303 [9 pages] (2013).

12. *Alfven Wave Collisions, The Fundamental Building Block of Plasma Turbulence III: Theory for Experimental Design*
Howes, G. G., Nielson, K. D., Drake, D. J., Schroeder, J. W. R., Skiff, F., Kletzing, C. A., and Carter, T. A.
Phys. Plasmas, **20**, 072304 [12 pages] (2013).

13. *Current Sheets and Collisionless Damping in Kinetic Plasma Turbulence*
TenBarge, J. M. and **Howes, G. G.**
Astrophys. J. Lett., **771**, L27 [6 pages] (2013).

14. *Toward Astrophysical Turbulence in the Laboratory*[1]
Howes, G. G., Drake, D. J., Nielson, K.D., Carter, T. A., Kletzing, C. A.,and Skiff, F.
Phys. Rev. Lett., **109**, 255001 (2012).

15. *Interpreting Magnetic Variance Anisotropy Measurements in the Solar Wind*
TenBarge, J. M., Podesta, J. J., Klein, K. G., and Howes, G. G.
Astrophys. J., **753**, 107 (2012).

16. *Evidence of Critical Balance in Kinetic Alfven Wave Turbulence Simulations*
TenBarge, J. M. and Howes, G. G.
Phys. Plasmas, **19**, 055901 (2012).

17. *A Weakened Cascade Model for Turbulence in Astrophysical Plasmas*
Howes, G. G., TenBarge, J. M., and Dorland, W.
Phys. Plasmas **18**, 102305 (2011).

18. *Prediction of the Proton-to-Total Turbulent Heating in the Solar Wind*
Howes, G. G.
Astrophys. J. **738**, 40 (2011).

19. *Gyrokinetic Simulations of Solar Wind Turbulence from Ion to Electron Scales*
Howes, G. G., TenBarge, J. M., Dorland, W., Quataert, E., Schekochihin, A. A., Numata, R., and Tatsuno, T.
Phys. Rev. Lett. **107**,035004 (2011).

20. *A prescription for the turbulent heating of astrophysical plasmas*
Howes, G. G.
Mon. Not. Roy. Astron. Soc. Lett. **409**, L104–L108 (2010).

21. *AstroGK: Astrophysical Gyrokinetics Code*
Numata, R., Howes, G. G., Tatsuno, T., Barnes, M., and Dorland, W.
J. Comp. Phys. **229**, 9347–9372 (2010).

[1]This publication was selected as an *Editor's Suggestion* in Physical Review Letters, was singled out as an example of a successful laboratory astrophysics project in a news article in Nature [*Lab astrophysics aims for the stars*, Reich, E. S, Nature **491**, 509 (2012)], and was highlighted in a Viewpoint in Physics, the APS publication that features commentary on the most important papers published by the Society [*Viewpoint: Turbulent Plasma in the Lab*, Gregori, G. and Reville, B., Physics, **5**, 141 (2012)].

References

[1] I. G. Abel, M. Barnes, S. C. Cowley, W. Dorland, and A. A. Schekochihin. Linearized model Fokker-Planck collision operators for gyrokinetic simulations. I. Theory. *Phys. Plasmas*, 15(12):122509–+, December 2008.

[2] O. Alexandrova, C. Lacombe, A. Mangeney, R. Grappin, and M. Maksimovic. Solar Wind Turbulent Spectrum at Plasma Kinetic Scales. *Astrophys. J.*, 760:121, December 2012.

[3] O. Alexandrova, J. Saur, C. Lacombe, A. Mangeney, J. Mitchell, S. J. Schwartz, and P. Robert. Universality of Solar-Wind Turbulent Spectrum from MHD to Electron Scales. *Phys. Rev. Lett.*, 103(16):165003–+, October 2009.

[4] M. Barnes, I. G. Abel, W. Dorland, D. R. Ernst, G. W. Hammett, P. Ricci, B. N. Rogers, A. A. Schekochihin, and T. Tatsuno. Linearized model Fokker-Planck collision operators for gyrokinetic simulations. II. Numerical implementation and tests. *Phys. Plasmas*, 16(7):072107–+, July 2009.

[5] J. E. Borovsky and M. H. Denton. No Evidence for Heating of the Solar Wind at Strong Current Sheets. *Astrophys. J. Lett.*, 739:L61, October 2011.

[6] C. H. K. Chen, T. S. Horbury, A. A. Schekochihin, R. T. Wicks, O. Alexandrova, and J. Mitchell. Anisotropy of Solar Wind Turbulence between Ion and Electron Scales. *Phys. Rev. Lett.*, 104(25):255002–+, June 2010.

[7] T. Dombre, U. Frisch, M. Henon, J. M. Greene, and A. M. Soward. Chaotic streamlines in the ABC flows. *J. Fluid Mech.*, 167:353–391, June 1986.

[8] D. J. Drake, J. W. R. Schroeder, G. G. Howes, C. A. Kletzing, F. Skiff, T. A. Carter, and D. W. Auerbach. Alfvén wave collisions, the fundamental building block of plasma turbulence. IV. Laboratory experiment. *Physics of Plasmas*, 20(7):072901, July 2013.

[9] N. N. Filonenko, R. Z. Sagdeev, and G. M. Zaslavsky. Destruction of Magnetic Surfaces by Magnetic Field Irregularities. 2. *Nuclear Fusion*, 7(4):253, 1967.

[10] E. A. Frieman and L. Chen. Nonlinear gyrokinetic equations for low-frequency electromagnetic waves in general plasma equilibria. *Phys. Fluids*, 25:502–508, March 1982.

[11] B. Guest and A. Shalchi. Random walk of magnetic field lines in dynamical turbulence: A field line tracing method. II. Two-dimensional turbulence. *Phys. Plasmas*, 19(3):032902, March 2012.

[12] D. R. Hatch, M. J. Pueschel, F. Jenko, W. M. Nevins, P. W. Terry, and H. Doerk. Origin of Magnetic Stochasticity and Transport in Plasma Microturbulence. *Phys. Rev. Lett.*, 108(23):235002, June 2012.

[13] D. R. Hatch, M. J. Pueschel, F. Jenko, W. M. Nevins, P. W. Terry, and H. Doerk. Magnetic stochasticity and transport due to nonlinearly excited subdominant microtearing modes. *Phys. Plasmas*, 20(1):012307, January 2013.

[14] G. G. Howes. Inertial range turbulence in kinetic plasmas. *Phys. Plasmas*, 15(5):055904, May 2008.

[15] G. G. Howes. A Unified Model of Astrophysical Plasma Turbulence. *Nature Comm.*, 2015. submitted.

[16] G. G. Howes, S. C. Cowley, W. Dorland, G. W. Hammett, E. Quataert, and A. A. Schekochihin. Astrophysical Gyrokinetics: Basic Equations and Linear Theory. *Astrophys. J.*, 651:590–614, November 2006.

[17] G. G. Howes, W. Dorland, S. C. Cowley, G. W. Hammett, E. Quataert, A. A. Schekochihin, and T. Tatsuno. Kinetic Simulations of Magnetized Turbulence in Astrophysical Plasmas. *Phys. Rev. Lett.*, 100(6):065004, February 2008.

[18] G. G. Howes, D. J. Drake, K. D. Nielson, T. A. Carter, C. A. Kletzing, and F. Skiff. Toward Astrophysical Turbulence in the Laboratory. *Phys. Rev. Lett.*, 109(25):255001, December 2012.

[19] G. G. Howes and K. D. Nielson. Alfvén wave collisions, the fundamental building block of plasma turbulence. I. Asymptotic solution. *Phys. Plasmas*, 20(7):072302, July 2013.

[20] G. G. Howes, K. D. Nielson, D. J. Drake, J. W. R. Schroeder, F. Skiff, C. A. Kletzing, and T. A. Carter. Alfvén wave collisions, the fundamental building block of plasma turbulence. III. Theory for experimental design. *Physics of Plasmas*, 20(7):072304, July 2013.

[21] G. G. Howes, J. M. TenBarge, W. Dorland, E. Quataert, A. A. Schekochihin, R. Numata, and T. Tatsuno. Gyrokinetic simulations of solar wind turbulence from ion to electron scales. *Phys. Rev. Lett.*, 107:035004, 2011.

[22] J. R. Jokipii and E. N. Parker. Random Walk of Magnetic Lines of Force in Astrophysics. *Phys. Rev. Lett.*, 21:44–47, July 1968.

[23] H. Karimabadi, V. Roytershteyn, M. Wan, W. H. Matthaeus, W. Daughton, P. Wu, M. Shay, B. Loring, J. Borovsky, E. Leonardis, S. C. Chapman, and T. K. M. Nakamura. Coherent structures, intermittent turbulence, and dissipation in high-temperature plasmas. *Phys. Plasmas*, 20(1):012303, January 2013.

[24] K. H. Kiyani, S. C. Chapman, Y. V. Khotyaintsev, M. W. Dunlop, and F. Sahraoui. Global scale-invariant dissipation in collisionless plasma turbulence. *Phys. Rev. Lett.*, 103:075006, 2009.

[25] T. C. Li, G. G. Howes, K. G. Klein, and J. M. TenBarge. Dissipation via Landau Damping in Two- and Three-Dimensional Plasma Turbulence. *Phys. Rev. Lett.*, 2015. submitted.

[26] J. Maron and P. Goldreich. Simulations of incompressible magnetohydrodynamic turbulence. *Astrophys. J.*, 554:1175–1196, 2001.

[27] W. M. Nevins, E. Wang, and J. Candy. Magnetic Stochasticity in Gyrokinetic Simulations of Plasma Microturbulence. *Phys. Rev. Lett.*, 106(6):065003, February 2011.

[28] K. D. Nielson, G. G. Howes, and W. Dorland. Alfvén wave collisions, the fundamental building block of plasma turbulence. II. Numerical solution. *Physics of Plasmas*, 20(7):072303, July 2013.

[29] R. Numata, G. G. Howes, T. Tatsuno, M. Barnes, and W. Dorland. AstroGK: Astrophysical gyrokinetics code. *J. Comp. Phys.*, 229:9347, 2010.

[30] S. A. Orszag and C.-M. Tang. Small-scale structure of two-dimensional magnetohydrodynamic turbulence. *J. Fluid Mech.*, 90:129–143, January 1979.

[31] K. T. Osman, W. H. Matthaeus, J. T. Gosling, A. Greco, S. Servidio, B. Hnat, S. C. Chapman, and T. D. Phan. Magnetic Reconnection and Intermittent Turbulence in the Solar Wind. *Phys. Rev. Lett.*, 112(21):215002, May 2014.

[32] K. T. Osman, W. H. Matthaeus, A. Greco, and S. Servidio. Evidence for Inhomogeneous Heating in the Solar Wind. *Astrophys. J. Lett.*, 727:L11+, January 2011.

[33] K. T. Osman, W. H. Matthaeus, B. Hnat, and S. C. Chapman. Kinetic Signatures and Intermittent Turbulence in the Solar Wind Plasma. *Phys. Rev. Lett.*, 108(26):261103, June 2012.

[34] K. T. Osman, W. H. Matthaeus, M. Wan, and A. F. Rappazzo. Intermittency and Local Heating in the Solar Wind. *Phys. Rev. Lett.*, 108(26):261102, June 2012.

[35] T. N Parashar, C. Salem, R. Wicks, H. Karimabadi, S. Gary, B. Chandran, and W. H Matthaeus. Turbulent Dissipation Challenge – Problem Description. *ArXiv e-prints*, May 2014.

[36] S. Perri, M. L. Goldstein, J. C. Dorelli, and F. Sahraoui. Detection of Small-Scale Structures in the Dissipation Regime of Solar-Wind Turbulence. *Phys. Rev. Lett.*, 109(19):191101, November 2012.

[37] A. B. Rechester and M. N. Rosenbluth. Electron heat transport in a Tokamak with destroyed magnetic surfaces. *Phys. Rev. Lett.*, 40:38–41, January 1978.

[38] A. Retinò, D. Sundkvist, A. Vaivads, F. Mozer, M. André, and C. J. Owen. In situ evidence of magnetic reconnection in turbulent plasma. *Nature Physics*, 3:236–238, April 2007.

[39] M. N. Rosenbluth, R. Z. Sagdeev, J. B. Taylor, and G. M. Zaslavsky. Destruction of magnetic surfaces by magnetic field irregularities. *Nuclear Fusion*, 6(4):297, 1966.

[40] F. Sahraoui, M. L. Goldstein, G. Belmont, P. Canu, and L. Rezeau. Three Dimensional Anisotropic k Spectra of Turbulence at Subproton Scales in the Solar Wind. *Phys. Rev. Lett.*, 105(13):131101–+, September 2010.

[41] F. Sahraoui, M. L. Goldstein, P. Robert, and Y. V. Khotyaintsev. Evidence of a Cascade and Dissipation of Solar-Wind Turbulence at the Electron Gyroscale. *Phys. Rev. Lett.*, 102(23):231102–+, June 2009.

[42] S. Servidio, W. H. Matthaeus, M. Wan, D. Ruffolo, A. F. Rappazzo, and S. Oughton. Complexity and Diffusion of Magnetic Flux Surfaces in Anisotropic Turbulence. *Astrophys. J.*, 785:56, April 2014.

[43] A. Shalchi. A Unified Particle Diffusion Theory for Cross-field Scattering: Subdiffusion, Recovery of Diffusion, and Diffusion in Three-dimensional Turbulence. *Astrophys. J. Lett.*, 720:L127–L130, September 2010.

[44] A. Shalchi, J. W. Bieber, W. H. Matthaeus, and G. Qin. Nonlinear Parallel and Perpendicular Diffusion of Charged Cosmic Rays in Weak Turbulence. *Astrophys. J.*, 616:617–629, November 2004.

[45] A. Shalchi and I. Kourakis. Analytical description of stochastic field-line wandering in magnetic turbulence. *Phys. Plasmas*, 14(9):092903, September 2007.

[46] P. L. Similon and R. N. Sudan. Energy dissipation of Alfven wave packets deformed by irregular magnetic fields in solar-coronal arches. *Astrophys. J.*, 336:442–453, January 1989.

[47] F. Skiff, D. A. Boyd, and J. A. Colborn. Measurements of electron parallel-momentum distributions using cyclotron wave transmission. *Phys. Fluids B*, 5:2445–2450, July 1993.

[48] B. U. O. Sonnerup and L. J. Cahill, Jr. Magnetopause Structure and Attitude from Explorer 12 Observations. *J. Geophys. Res.*, 72:171, January 1967.

[49] K. H. Spatschek. Aspects of stochastic transport in laboratory and astrophysical plasmas. *Plasma Phys. Con. Fus.*, 50(12):124027, December 2008.

[50] D. Sundkvist, A. Retinò, A. Vaivads, and S. D. Bale. Dissipation in Turbulent Plasma due to Reconnection in Thin Current Sheets. *Phys. Rev. Lett.*, 99(2):025004, July 2007.

[51] J. M. TenBarge, W. Daughton, H. Karimabadi, G. G. Howes, and W. Dorland. Collisionless reconnection in the large guide field regime: Gyrokinetic versus particle-in-cell simulations. *Phys. Plasmas*, 21(2):020708, 2014.

[52] J. M. TenBarge and G. G. Howes. Current Sheets and Collisionless Damping in Kinetic Plasma Turbulence. *Astrophys. J. Lett.*, 771:L27, July 2013.

[53] J. M. TenBarge, G. G. Howes, and W. Dorland. Collisionless Damping at Electron Scales in Solar Wind Turbulence. *Astrophys. J.*, 774:139, September 2013.

[54] J. M. TenBarge, G. G. Howes, W. Dorland, and G. W. Hammett. An oscillating Langevin antenna for driving plasma turbulence simulations. *Comp. Phys. Comm.*, 185:578–589, February 2014.

[55] D. J. Thuecks, F. Skiff, and C. A. Kletzing. Measurements of parallel electron velocity distributions using whistler wave absorption. *Rev. Sci. Instr.*, 83(8):083503, 2012.

[56] M. Wan, W. H. Matthaeus, H. Karimabadi, V. Roytershteyn, M. Shay, P. Wu, W. Daughton, B. Loring, and S. C. Chapman. Intermittent Dissipation at Kinetic Scales in Collisionless Plasma Turbulence. *Phys. Rev. Lett.*, 109(19):195001, November 2012.

[57] X. Wang, C. Tu, J. He, E. Marsch, and L. Wang. On Intermittent Turbulence Heating of the Solar Wind: Differences between Tangential and Rotational Discontinuities. *Astrophys. J. Lett.*, 772:L14, August 2013.

[58] Y. Wang, S. Boldyrev, and J. C. Perez. Residual Energy in Magnetohydrodynamic Turbulence. *Astrophys. J. Lett.*, 740:L36, October 2011.

[59] P. Wu, S. Perri, K. Osman, M. Wan, W. H. Matthaeus, M. A. Shay, M. L. Goldstein, H. Karimabadi, and S. Chapman. Intermittent Heating in Solar Wind and Kinetic Simulations. *Astrophys. J. Lett.*, 763:L30, February 2013.

[60] V. Zhdankin, S. Boldyrev, J. C. Perez, and S. M. Tobias. Energy Dissipation in Magnetohydrodynamic Turbulence: Coherent Structures or "Nanoflares"? *Astrophys. J.*, 795:127, November 2014.

[61] V. Zhdankin, D. A. Uzdensky, J. C. Perez, and S. Boldyrev. Statistical Analysis of Current Sheets in Three-dimensional Magnetohydrodynamic Turbulence. *Astrophys. J.*, 771:124, July 2013.